Elastic-Plastic Fracture Mechanics Analysis of a CT-Specimen - a Two-Dimensional Approach

Larsen, Gunner Chr.

Publication date:
1986

Document Version
Publisher's PDF, also known as Version of record

RISØ-M-2586

ELASTIC-PLASTIC FRACTURE MECHANICS ANALYSIS OF A CT-SPECIMEN - A TWO-DIMENSIONAL APPROACH

Gunner C. Larsen

Abstract. This report documents the results obtained from an elastic-plastic finite-element analysis of a compact tension specimen. The geometry of the model has been slightly modified compared to the physical specimen, but this is not considered to influence the results.

The analysis comprises a plane strain as well as a plane stress approximation. The results presented include applied loads and displacements at certain locations. Moreover, the J-integral and the crack opening displacement have been presented.

The plane strain and the plane stress approximation have been compared and the plane stress approximation is believed to deliver the best results. The results have been obtained using the finite-element code ADINA and the postprocessor code JINT.

June 1986
Risø National Laboratory, DK-4000 Roskilde, Denmark

ISBN 87-550-1231-0
ISSN 0418-6435

Grafisk Service, Risø 1986

CONTENTS

page

1. INTRODUCTION 5

2. DESCRIPTION OF THE PHYSICAL SYSTEM 5

3. DESCRIPTION OF THE FINITE-ELEMENT FORMULATION 6
   3.1 Finite-element mesh 7
   3.2 Material data 9
   3.3 Boundary conditions 9
   3.4 Loading 9
   3.5 Solution strategy 9

4. DETERMINATION OF COD AND J-INTEGRALS 10

5. RESULTS 14

6. CONCLUSIONS 21

REFERENCES 23

1. INTRODUCTION

This report comprises the first part of Risø's contribution to a Nordic Round Robin on fracture mechanics within the framework of the NKA collaboration. The participants in this numerical exercise are

- Veritas Research, Norway
- KTH, Sweden
- Technical Research Center of Finland
- Risø National Laboratory, Denmark.

The problem to be dealt with is a two-dimensional finite-element analysis of a compact tension (CT) specimen exposed to displacements of the load pin holes.

2. DESCRIPTION OF THE PHYSICAL SYSTEM

The specimen to be dealt with in this calculation is the compact tension specimen shown in Fig. 1 below. Values of the geometric quantities are given in Table 1.

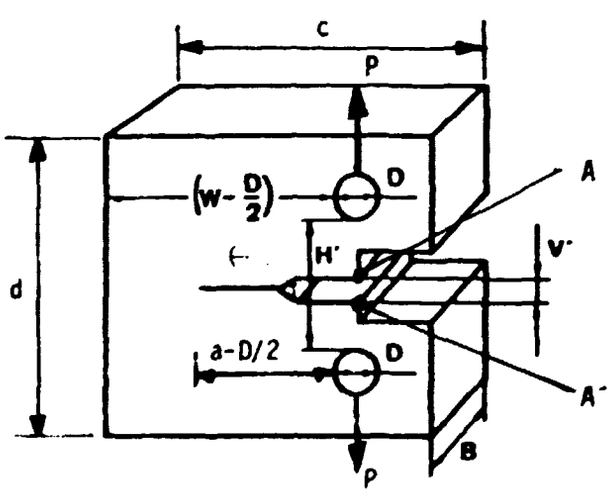

Fig. 1. CT-specimen.

Table 1. Dimensions of the specimen in [mm]

W	a	B	B_{net}	D	c	d	H'	V'
50.35	27.713	25	20	12.5	62.5	60	25.5	3.5

The angle θ has not been specified, however, it is established from Fig. 1 to 60^{0}. The material shows an elastic-plactic behaviour, and the stress-strain relationship has been obtained from laboratory tests (1). In the linear region E^{I} = 200 GPa. In the nonlinear region the relation between strain (ε) and stress (σ) appears from Table 2 below.

Table 2. Stress-strain relationship

ε[%]	0.1070	0.3295	0.6945	1.1595	7.7095	18.71
σ[MPa]	214	259	289	319	446	500

Poisson's ratio ν is 0.3.

3. DESCRIPTION OF THE FINITE-ELEMENT FORMULATION

The finite-element codes used in the numerical analysis are the 1981 and 1985 versions of the ADINA code. Furthermore, the 1984 and 1985 versions of the preprocessor code ADINA-IN have been used for the generation of input data and, finally, the 1985 version of the postprocessor code ADINA-PLOT has been used for the

generation of graphic output. The codes are documented in (2-6). All options used in the calculations are standard ADINA options. The solution details are presented in the following sections.

3.1. Finite-element mesh

In the numerical model the geometry has been slightly changed compared to the physical geometry shown in Fig. 1 as the load pin holes are not modelled, and neither is part of the specimen beyond the load point. This simplification is not considered to effect the stress distribution around the crack. Furthermore, only one half of the specimen is modelled due to symmetry in geometry as well as in load. The resulting finite-element mesh is shown in Fig. 2.

Two groups of elements have been defined. Group I is materially nonlinear and contains 29 eight-noded isoparameteric plane elements with nine integration points in each element. All the elements in this group are quadrilaterals except the elements 1-4 at the crack tip which are degenerated to triangular shape.

In all the elements of this group the side nodes have been placed at the mid points which means that the configuration around the crack tip possesses the appropriate 1/r singularity for plastic calculations (7).

Group II of the elements is materially linear and consists of one truss element with two integration points and a cross section area of 1 mm^2. This element is adopted in order to obtain the reaction force, P, at node 112 for a prescribed displacement at this node.

The total system consists of 217 equations with a maximum half bandwidth of 75. The mean half bandwidth is 25.

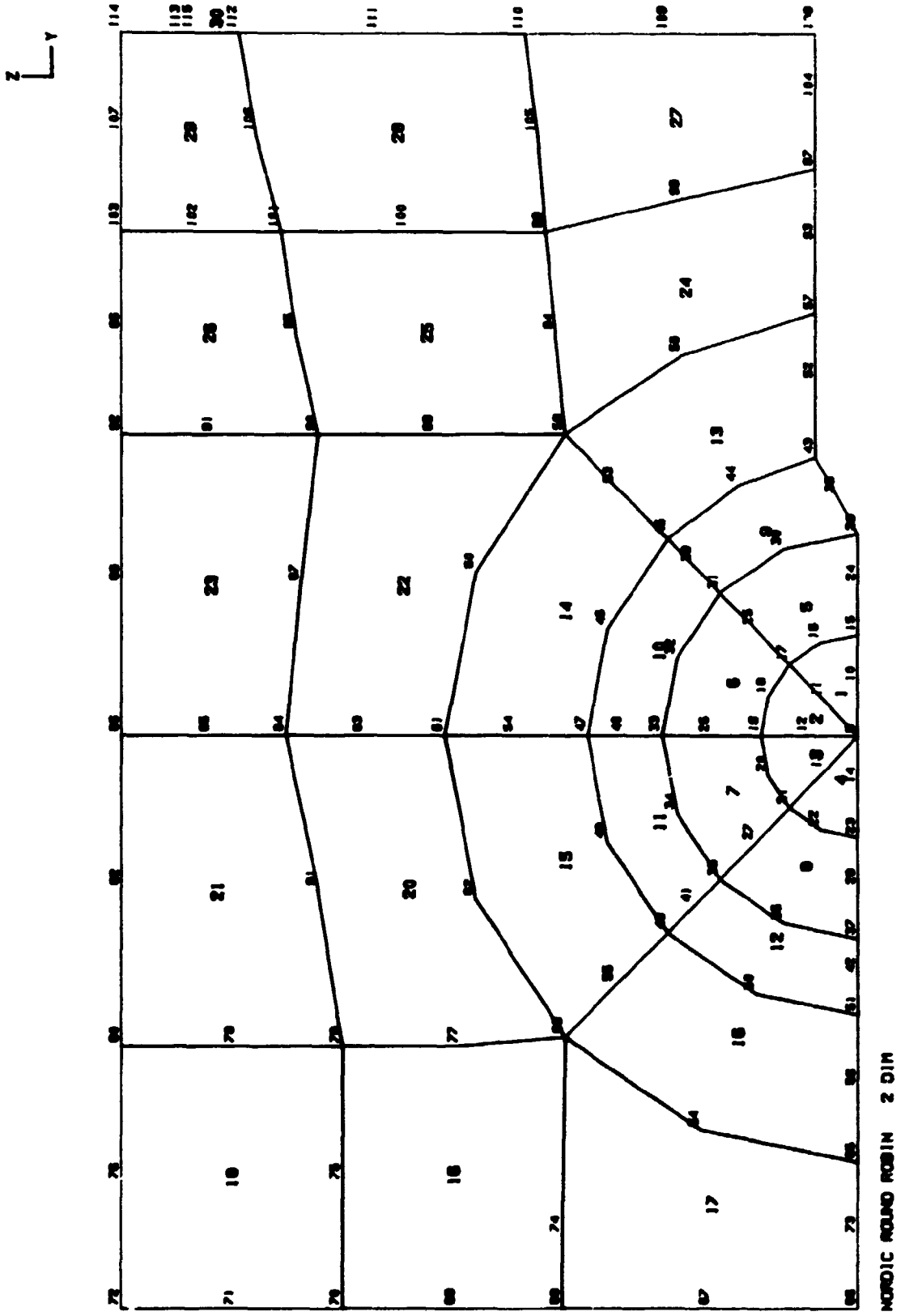

Fig. 2. Finite-element mesh.

3.2. Material data

The constitutive model for the nonlinear material in group I of the elements is specified as a multilinear elastic-plastic model with von Mises yield condition and based on the stress-strain relationship given in Table 2 and Poisson's ratio equal to 0.3. In order to avoid numerical difficulties in the computations the values in Table 2 have been supplemented with the stress-strain point

$$\varepsilon = 500\%, \quad \sigma = 1000 \text{ MPa}.$$

The linear material in group II of the elements is described by a Young's modulus $E^{II} = 10^7$ GPa.

3.3. Boundary conditions

Symmetry boundary conditions are imposed on the nodes 1-10, 66, 73, 65, 56, 51, 42, 37, 28, 23, 14, 15, 24, 28, 38, 43, 52, 57, 93, 97, 104, and 108. Moreover, node 66 is fixed in space.

3.4. Loading

The load is introduced by prescribing the displacement at node 112. A linear incrementation scheme is adopted and the maximum displacement $\Delta V_{108} = 1.05$ mm, corresponding to $V_2 = 2.1$ mm (V_2 denotes the displacement between the load points), is obtained in 21 steps.

3.5. Solution strategy

Since the physical problem essentially is a three-dimensional problem both a plane strain analysis and a plane stress analysis (group I of the elements) have been performed in order to obtain upper and lower bounds for the results and to compare these.

The nonlinear geometry option in ADINA is not used in the present analysis as a small displacement and a small strain formulation are used.

However, the materially nonlinear effects require incrementation of the load and a subsequent reformation of the stiffness matrix and quilibrium iterations at each load step. The modified Newton algorithm was used in the equilibrium iterations, and convergence to the specified degree of accuracy has been obtained within between 1 and 3 iterations.

Each type of analysis requires two ADINA calculations due to temporary incompatibilities in the programme package. One calculation, based on the 1981 version of ADINA, is carried out at a Burroughs B7800 computer. This calculation is performed in Burroughs single precision corresponding to an accuracy of 11-12 significant figures and generate the input data for the J-integral calculation. The second calculation based on the 1985 version of ADINA is carried out at an APOLLO installation. This calculation is performed in IBM double precision corresponding to an accuracy of 14-15 significant figures and generates the input for the graphic postprocessor ADINA-PLOT.

4. DETERMINATION OF COD AND THE J-INTEGRAL

Determination of the crack opening displacement (COD) requires plots of the deformed configuration at each load step. Based on these plots the COD is evaluated using the method of extrapolation lines as illustrated in Fig. 3. The COD values are presented in the next section. Note that the values presented correspond to a crack opening displacement of a "half crack".

The J-integral is evaluated using the postprocessor code JINT described in (8). The integrations have been performed over six different areas. These are described in Figs. 4-9.

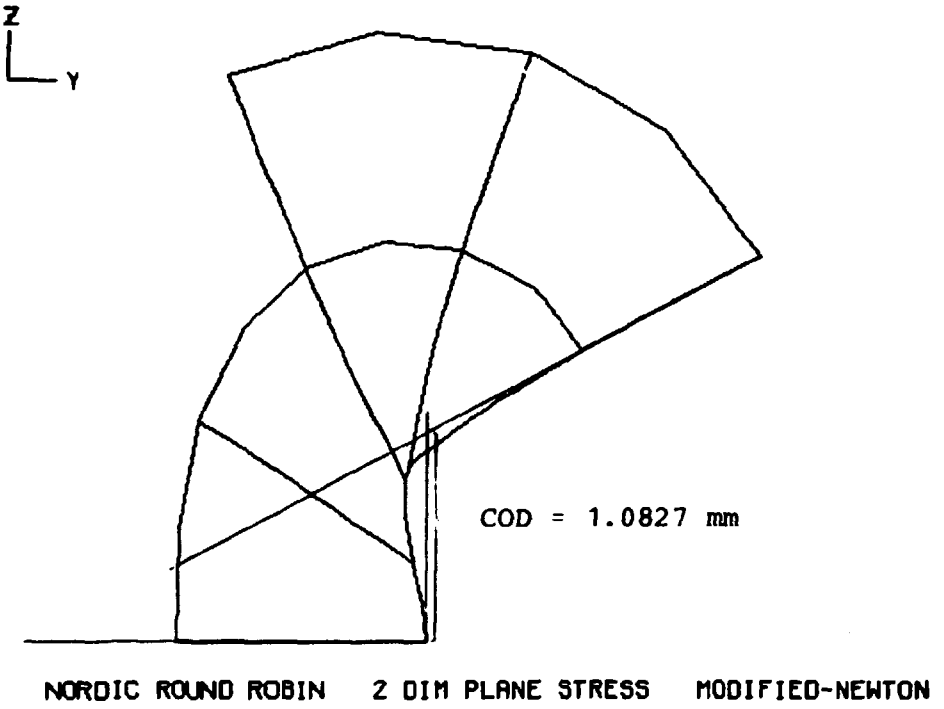

Fig. 3. COD at load step 10.

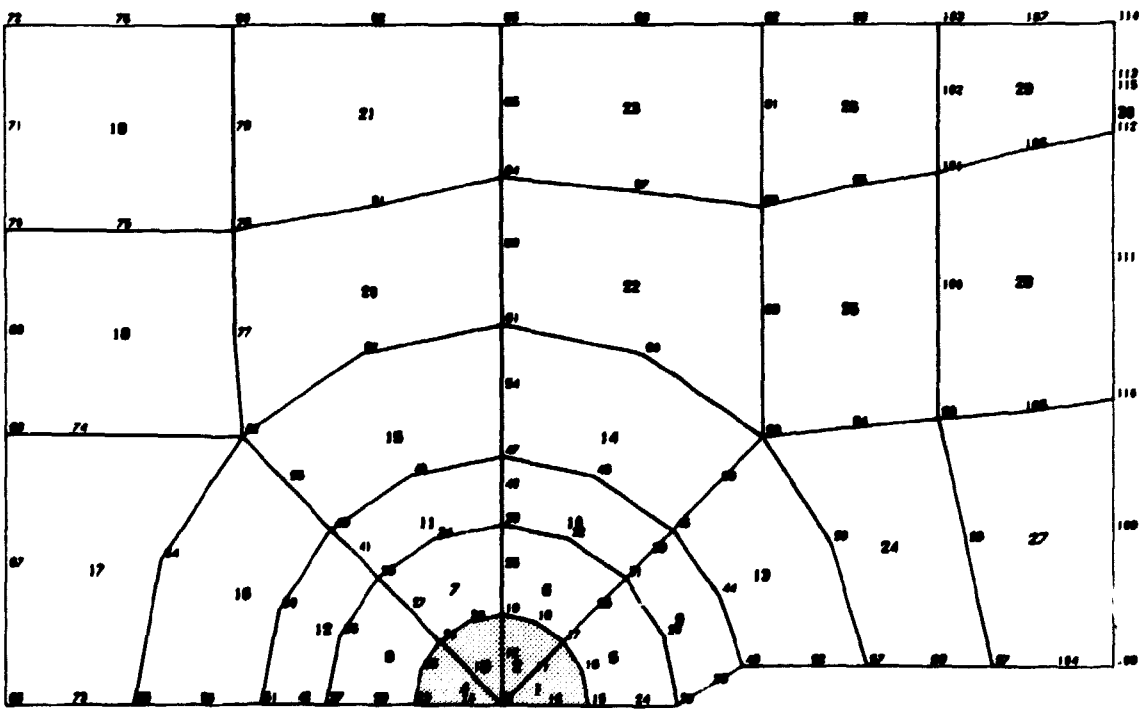

Fig. 4. Integration area No. 1.

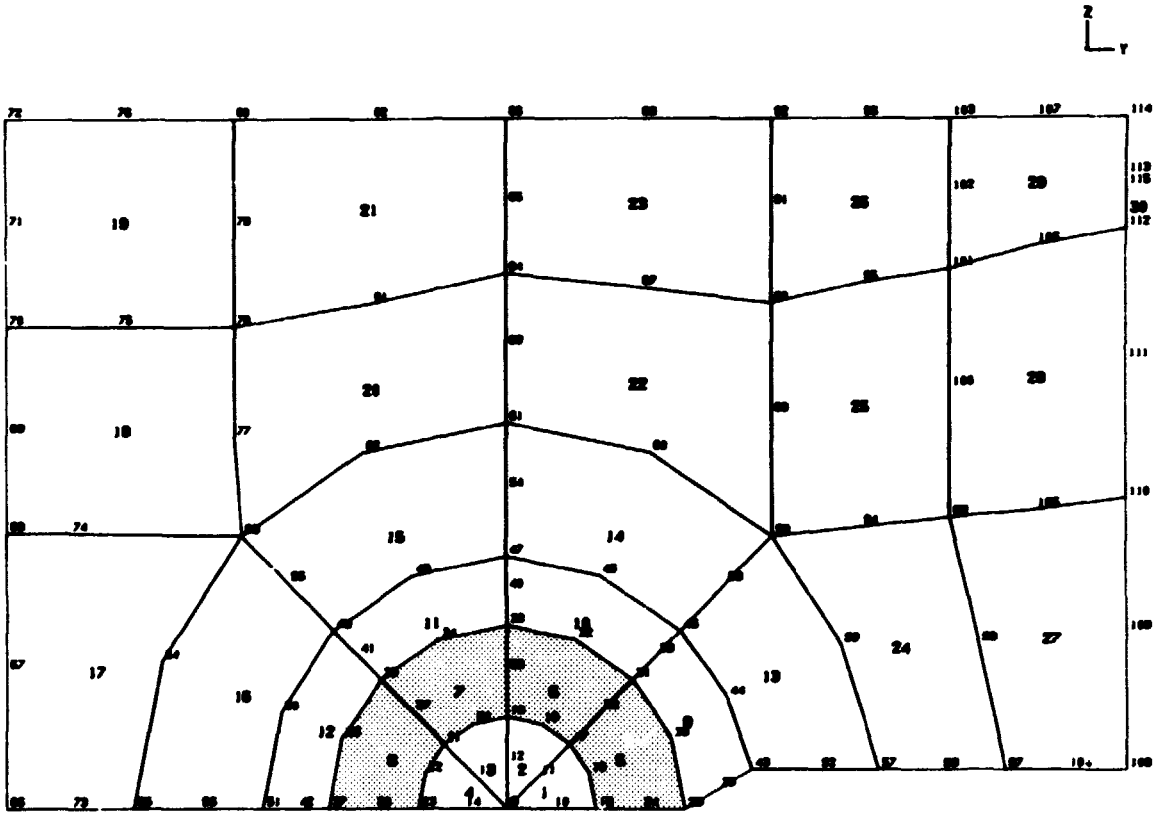

Fig. 5. Integration No. 2.

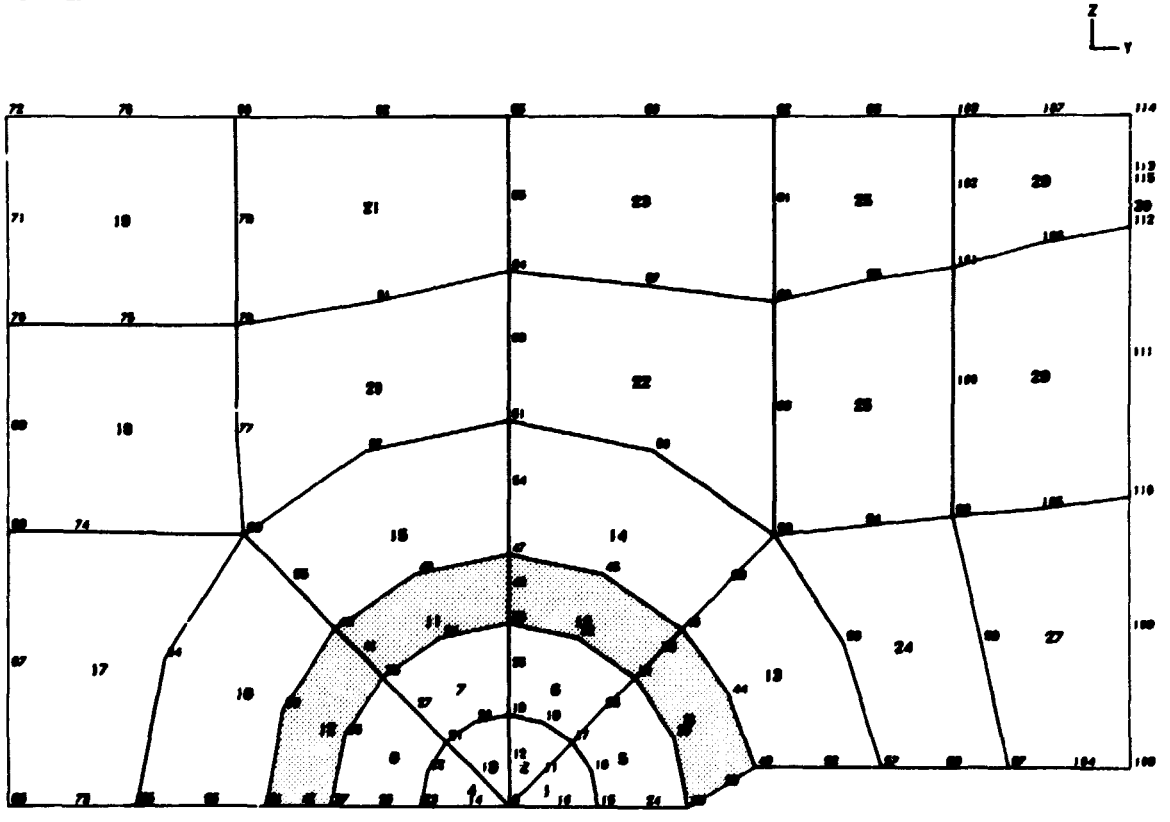

Fig. 6. Integration No. 3.

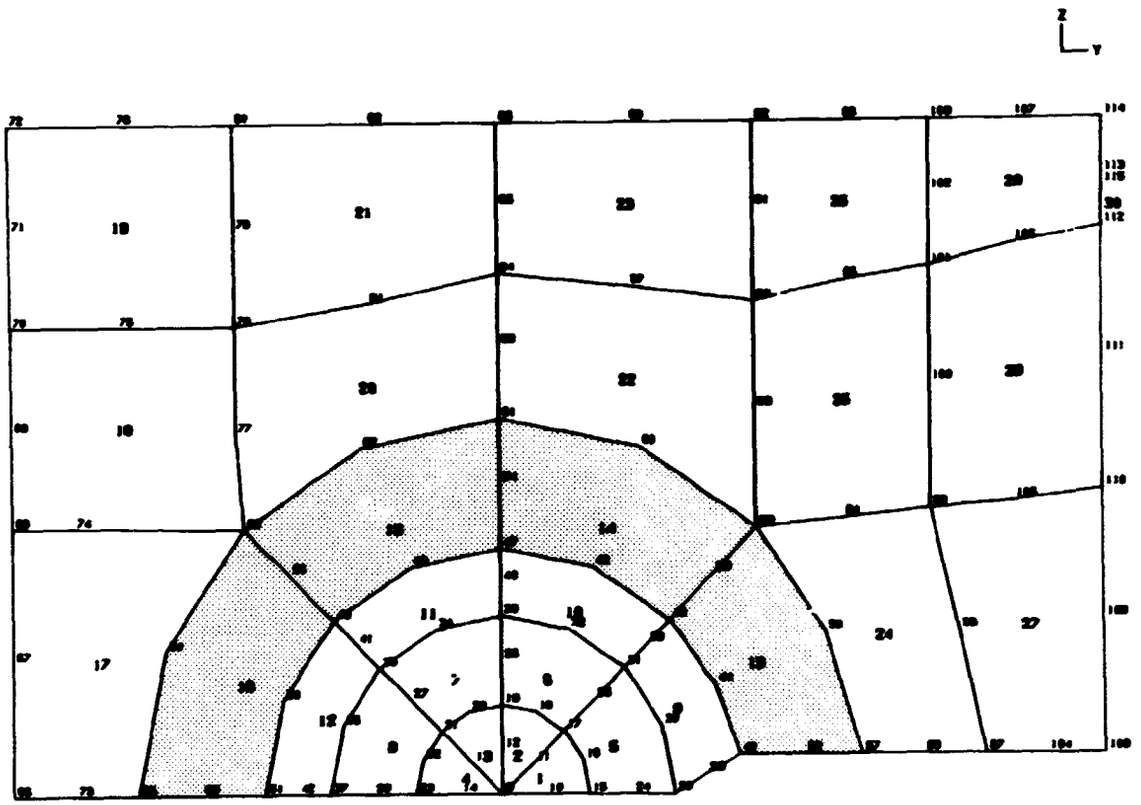

Fig. 7. Integration No. 4.

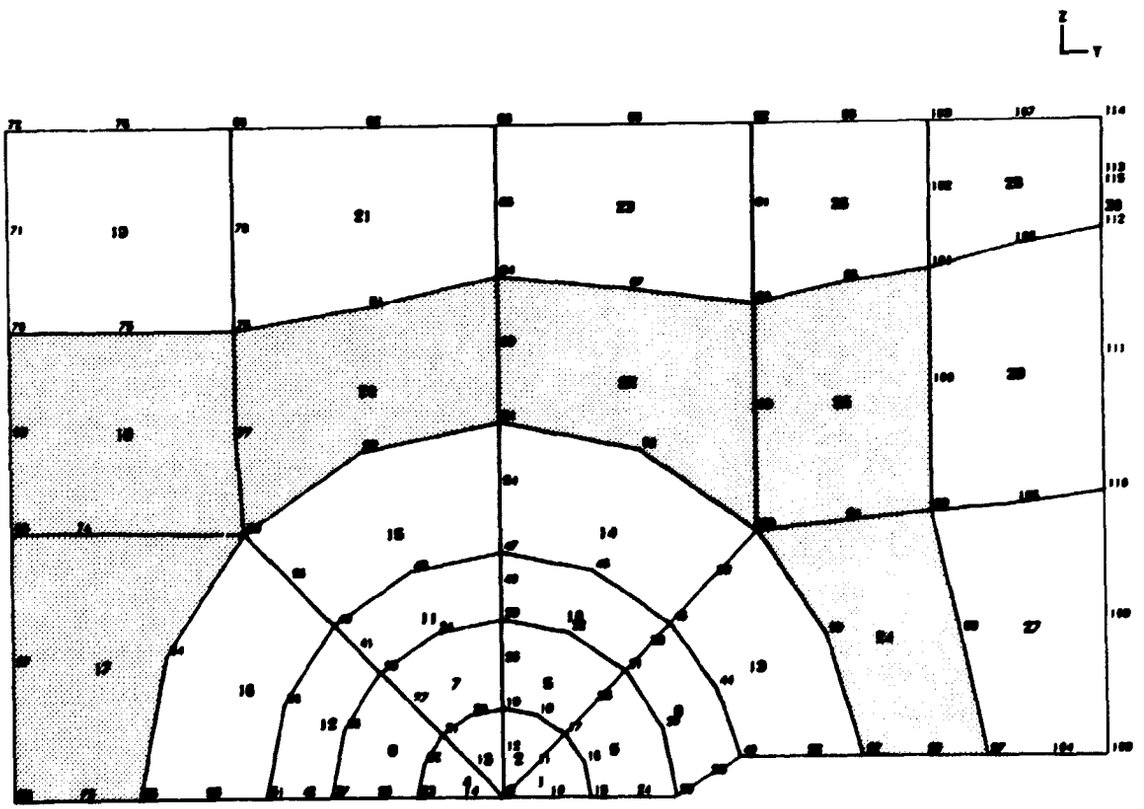

Fig. 8. Integration No. 5.

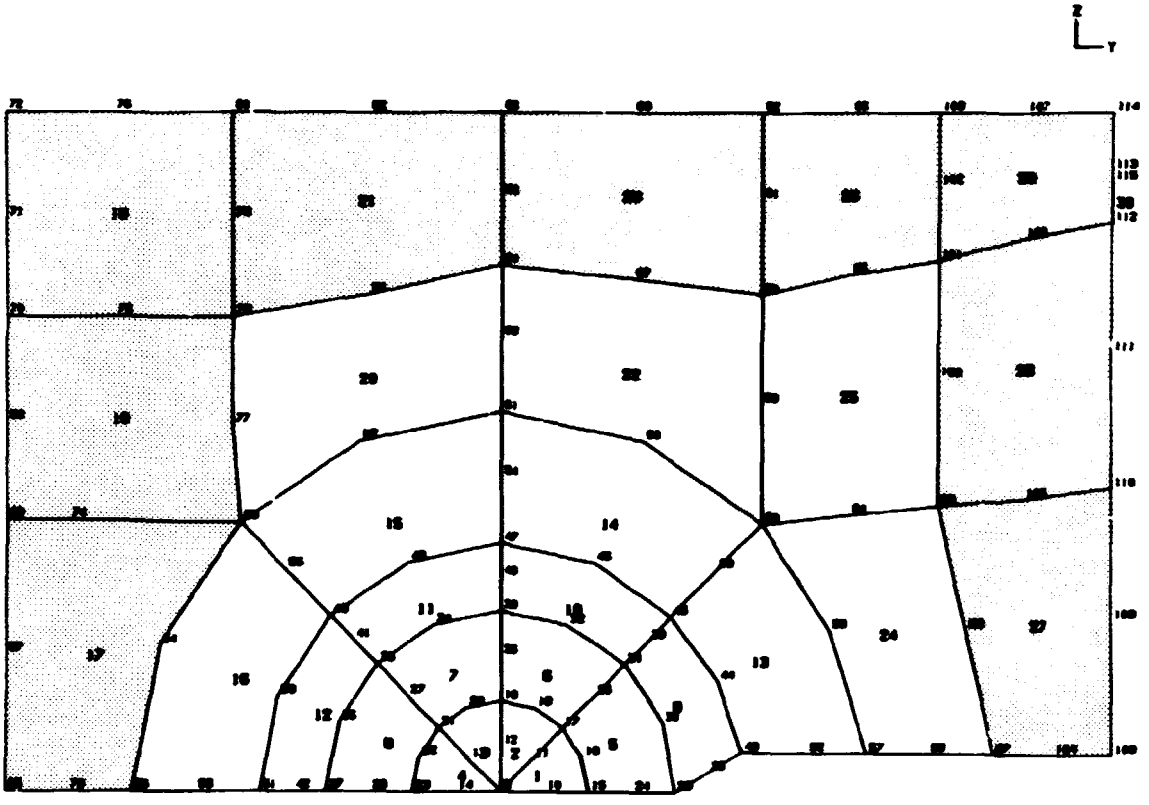

Fig. 9. Integration No. 6.

The results from the calculations are described in Section 5.

5. RESULTS

The results obtained in the analysis are presented in the attached tables and figures. The solution characteristics have been described in Section 3 and are further elaborated in Table 3. The results covering the plain strain approximation are given in the Tables 4-5 where V_1 denotes the displacement between the points A_1 and A_2 in Fig. 1, V_2 denotes the displacement between the load points and P denotes the reaction force at node 112. J_i symbolize the J-integral corresponding to integration area No. i. The average integral $\overline{J}$ is calculated as the arithmetic mean of the J-values corresponding to the integration areas 2-4. This procedure is considered to give the most appropriate mean value as "disturbances"

from the crack tip and the outer boundary are avoided. v denotes the coefficient of variation corresponding to $\overline{J}$. The results concerning the plane stress approximation are given in the Tables 6-7 where the same notation is adopted.

Finally, P, $\overline{J}$ and COD are plotted as a function of V_1 in Figs. 10-12 for both the plane strain and the plane stress approximation. In the plane strain approximation P is taken as 20 times the reaction force in node 112 in order to obtain reaction forces of the same order of magnitude as in the plane stress approximation. This is due to the fact that the thickness of the specimen in the plane stress approximation is taken to 20 times the thickness of the specimen in the plane strain approximation. The displacement V_1 has been chosen as the characteristic deformation in order to avoid the local deformations which are included in V_2.

Table 3. Solution characteristics

Type of analysis	2 D
Computer	Burroughs B7800
Code	ADINA
Type of elements	8-node, plane isoparametric element 2-node truss element
No.of DOF's	217
No. of elements	29 + 1
No. of nodal points	115
Conv. criteria	energy criterion
Conv. tolerance	$1 \cdot 10^3$
No. of loading steps	21
Method of calc. J	described in (8)
Method of calc. COD	extrapolation lines

Table 4. Displacements, reaction forces and COD for the plane strain approximation.

Step No.	V_1 mm	V_2 mm	P kN	P×20 kN	COD mm
1	0.089679	0.099999	0.4205	8.4100	0.0406
2	0.179742	1.999999	0.8103	16.2600	0.0888
3	0.269972	0.300000	1.1094	22.1880	0.1687
4	0.361480	0.400000	1.2710	25.4200	0.2650
5	0.455768	0.500000	1.3642	27.2840	0.3648
6	0.550452	0.600000	1.4428	28.8560	0.4743
7	0.645836	0.700000	1.5053	30.1060	0.5872
8	0.740366	0.800000	1.5588	31.1760	0.7048
9	0.835544	0.900000	1.6044	32.0880	0.8109
10	0.930800	1.000000	1.6444	32.8880	0.9063
11	1.025912	1.100000	1.6795	33.5900	1.0233
12	1.121484	1.200000	1.7114	34.2280	1.1413
13	1.217308	1.300000	1.7413	34.8260	1.2430
14	1.313074	1.400000	1.7697	35.3940	1.3448
15	1.408440	1.500000	1.7964	35.9280	1.4623
16	1.503988	1.600000	1.8205	36.4100	1.6017
17	1.599704	1.700000	1.8435	36.8700	1.6772
18	1.695410	1.800000	1.8655	37.3100	1.7808
19	1.791088	1.900000	1.8866	37.7320	1.8816
20	1.886860	2.000000	1.9071	38.1420	2.0207
21	1.982846	2.100000	1.9264	38.5280	2.1261

Table 5. J-Integral results for the plane strain approximation.

Load step	J1 (N/mm)	J2 (N/mm)	J3 (N/mm)	J4 (N/mm)	J5 (N/mm)	J6 (N/mm)	$\bar{J}$ (N/mm)	v (%)
1	2.008	2.060	2.067	2.079	2.035	2.069	2.069	0.5
2	7.915	8.037	8.065	8.111	7.932	8.054	8.071	0.5
3	16.85	17.19	17.35	17.48	17.06	17.28	17.34	0.7
4	27.87	28.57	28.69	28.90	28.27	28.52	28.72	0.6
5	40.64	41.16	41.46	41.75	40.72	41.02	41.46	0.7
6	54.55	54.72	55.16	55.58	54.00	54.37	55.15	0.8
7	69.06	68.68	69.32	70.03	67.76	68.25	69.34	1.0
8	84.09	83.05	83.97	84.93	81.98	82.38	83.98	1.1
9	99.51	97.81	98.96	100.2	96.48	96.88	98.99	1.2
10	115.1	112.7	114.2	115.9	111.3	111.6	114.3	1.4
11	131.1	128.0	129.7	131.8	126.2	126.5	129.8	1.5
12	147.5	143.6	145.6	148.1	141.4	141.7	145.8	1.5
13	164.2	159.5	161.7	164.7	156.8	157.0	162.0	1.6
14	181.2	175.7	178.2	181.6	172.3	172.5	178.5	1.7
15	198.6	192.0	194.7	198.7	187.9	188.0	195.1	1.7
16	216.4	208.6	211.4	215.9	203.6	203.6	212.0	1.7
17	234.4	225.4	228.2	233.3	219.4	219.3	229.0	1.7
18	252.6	242.3	245.2	251.0	235.4	235.0	246.2	1.8
19	270.9	259.4	262.5	268.8	251.5	250.8	263.6	1.8
20	289.4	276.6	279.8	286.8	267.5	266.6	281.1	1.9
21	308.3	294.1	297.4	305.1	283.8	282.6	298.9	1.9

Table 6. Displacements, reaction forces and COD for the plane stress approximation.

Step No.	V_1 mm	V_2 mm	P kN	COD mm
1	0.0898566	0.0999974	7.4284	0.0435
2	0.1818166	0.1999952	13.2049	0.1230
3	0.2750660	0.2999940	16.6864	0.2260
4	0.3708120	0.3999940	18.7732	0.3443
5	0.4671260	0.4999920	20.0532	0.4550
6	0.5630860	0.5999920	20.9770	0.5803
7	0.6598180	0.6999920	21.7190	0.7000
8	0.7568840	0.7999920	22.3347	0.8323
9	0.8541880	0.8999920	22.8970	0.9479
10	0.9513400	0.9999920	23.3904	1.0827
11	1.0485040	1.0999920	23.8320	1.2088
12	1.1461320	1.1999920	24.2081	1.3157
13	1.2438200	1.2999920	24.5735	1.4580
14	1.3416900	1.3999920	24.9100	1.5960
15	1.4397540	1.4999900	25.2160	1.7515
16	1.5378400	1.5999900	25.4988	1.8453
17	1.6357080	1.6999900	25.7651	1.9320
18	1.7335760	1.7999900	26.0105	2.0862
19	1.8312440	1.8999900	26.2374	2.2413
20	1.9291880	1.9999900	26.4467	2.3653
21	2.0271400	2.1000000	26.6530	2.4732

Table 7. J-Integral results for the plane stress approximation.

Load step	J1 (N/mm)	J2 (N/mm)	J3 (N/mm)	J4 (N/mm)	J5 (N/mm)	J6 (N/mm)	$\bar{J}$ (N/mm)	v (%)
1	1.729	1.837	1.843	1.893	1.814	1.846	1.844	0.4
2	6.436	6.812	6.834	6.866	6.707	6.829	6.837	0.4
3	13.45	13.74	13.93	13.99	13.63	13.83	13.89	0.9
4	21.87	22.26	22.54	22.66	22.03	22.36	22.49	0.9
5	31.20	31.63	31.76	32.04	31.29	31.75	31.81	0.7
6	41.06	41.59	41.81	41.87	40.87	41.48	41.75	0.4
7	51.48	51.89	52.19	52.19	50.96	51.72	52.09	0.3
8	62.32	62.60	62.84	62.95	61.36	62.29	62.80	0.3
9	73.57	73.61	73.97	74.01	72.05	73.16	73.86	0.3
10	85.01	84.86	85.29	85.28	83.01	84.33	85.14	0.3
11	96.79	96.36	96.79	96.87	94.14	95.63	96.67	0.3
12	109.0	108.1	108.5	108.6	105.5	107.2	108.4	0.2
13	121.4	120.1	120.5	120.6	117.1	118.9	120.4	0.2
14	134.1	132.4	132.8	132.8	128.8	130.8	132.7	0.2
15	146.7	144.8	145.2	145.1	140.7	142.7	145.0	0.1
16	159.5	157.2	157.7	157.5	152.6	154.8	157.5	0.2
17	172.5	169.9	170.3	170.0	164.6	166.9	170.1	0.1
18	185.7	182.6	183.0	182.6	176.6	179.0	182.7	0.1
19	199.1	195.5	195.8	195.3	188.7	191.2	195.5	0.1
20	212.7	208.5	208.8	208.1	201.0	203.5	208.5	0.2
21	226.6	221.7	221.9	221.1	213.3	215.9	221.6	0.2

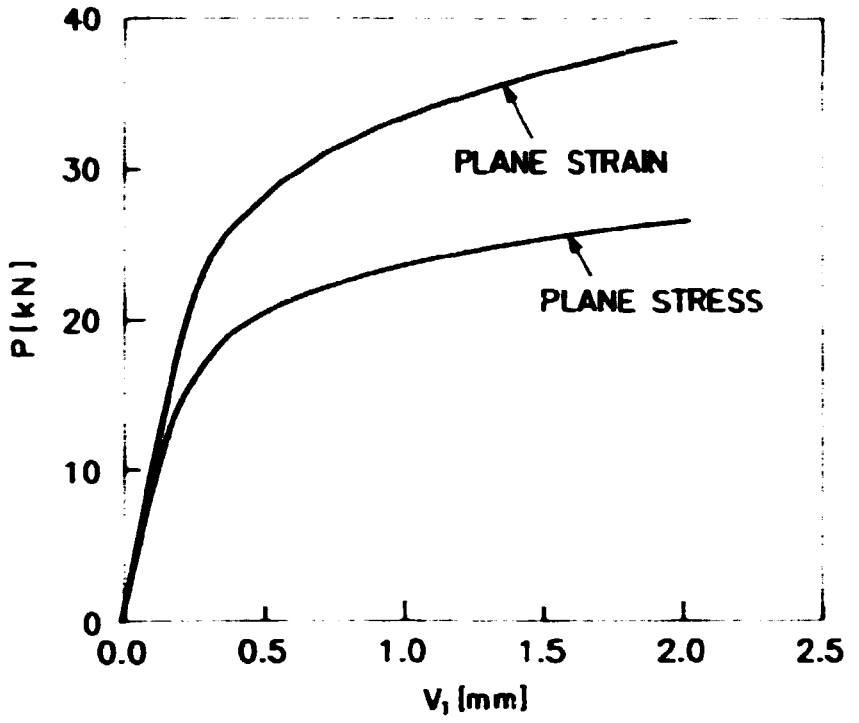

Fig. 10. P as a funcion of V_1.

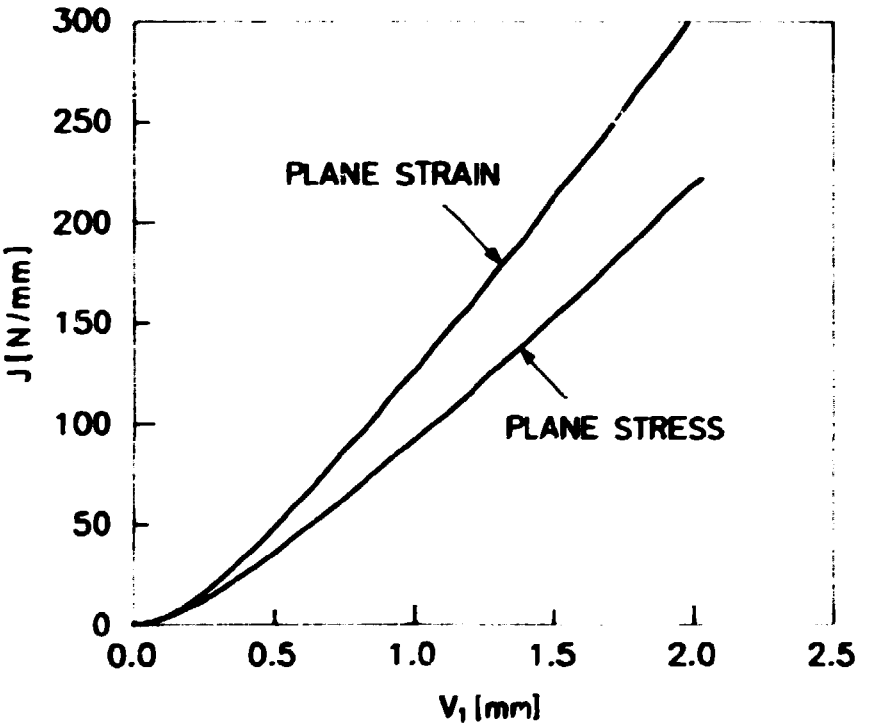

Fig. 11. $\bar{J}$ as a function of V_1.

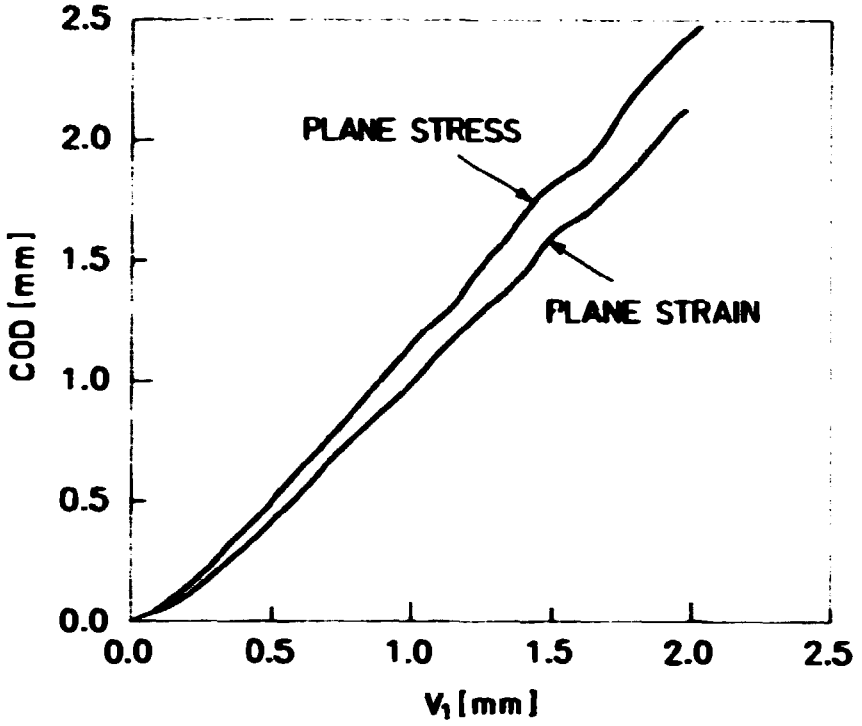

Fig. 12. COD as a function of V_1.

6. CONCLUSIONS

A lower and an upper bound solution characterized by a plane stress and a plain strain approximation, respectively, have been obtained.

The difference in stiffness in the plane strain and the plane stress situation is reflected both locally (COD) and globally (J,P) in the CT-specimen.

It is believed that the plane stress approximation is superior to the plain strain approximation. This is based on (7) and (9).

In (9) a specimen comparable to the one analysed in this report has been investigated using both two-dimensional plane strain and two-dimensional plane stress approximations. These results

have been compared to three-dimensional calculations and test results. The three-dimensional calculations and the test results showed up to be in close agreeement, and comparisons with the two-dimensional calculations showed that the plane stress situation gave the best description.

In (7) a related analysis has been made for another geometry. The specimen is here a bar subjected to three-point bending. Two-dimensional plane strain and plane stress calculations have been performed and compared to test results. Also for this geometry the test results showed up to be in closest agreement with the plane stress results.

Reverting to the present calculations it appears that the coefficient of variation of the J-integral seems to be smaller for the plane stress approximation compared to the plane strain approximation. This indicates a more consistent representation of the J-integral in the plane stress situation as this coefficient of variation ideally equals zero. This implies that the plane stress approximation is superior to the plane strain approximation for the present geometry.

REFERENCES

(1) TALJA, M. (1986), VTT, Helsinki, Private Communication.

(2) ADINA-IN, User's Manual, Report AE 83-6, ADINA Engineering, December 1984.

(3) ADINA-IN, User's Manual, Report AE 84-6, ADINA Engineering, December 1984.

(4) ADINA-IN, User's Manual, Report AE 81-1, ADINA Engineering, September 1981.

(5) ADINA-IN, User's Manual, Report AE 84-1, ADINA Engineering, December 1984.

(6) ADINA-PLOT, User's Manual, Report AE 84-3, ADINA Engineering, December 1984.

(7) de Lorenzi, H.G. and SHIH, C.F., Application of ADINA to Elastic-Plastic Fracture Problems. Prodeedings of the ADINA Conference, August 1977, Rep. 82448-6, MIT, Cambridge Mass., August 1977.

(8) LARSEN, G. (1985). Elastic-Plastic Finite-Element Analysis of a CT-Specimen like Geometry, Risø-I-182.

(9) HAMMEL, J.W. et al. (1981). An Elastic-Plastic finite-element analysis of a CT fracture specimen, Computers & Structures, Vol. 13, 757-770.

Riso National Laboratory

Riso - M - 2586

ELASTIC-PLASTIC FRACTURE MECHANICS ANALYSIS OF A CT-SPECIMEN - A TWO-DIMENSIONAL APPROACH

Gunner C. Larsen

Date 12 June 1986

Department or group
Meteorology and Wind Energy

Groups own registration number(s)

Project/contract no.

Pages 23 Tables 7 Illustrations 12 References 9

ISBN 87-550-1231-0

Abstract (Max. 2000 char.)

This report documents the results obtained from an elastic-plastic finite-element analysis of a compact tension specimen. The geometry of the model has been slightly modified compared to the physical specimen, but this is not considered to influence the results.

The analysis comprises a plane strain as well as a plane stress approximation. The results presented include applied loads and displacements at certain locations. Moreover, the J-integral and the crack opening displacement have been presented.

The plane strain and the plane stress approximation have been compared and the plane stress approximation is believed to deliver the best results. The results have been obtained using the finite-element code ADINA and the postprocessor code JINT.

Descriptors - EDB:

A CODES; CRACKS; ELASTICITY; FINITE-ELEMENT METHOD; FRACTURE MECHANICS; J CODES; PLASTICITY; STRAINS; STRESSES; TWO-DIMENSIONAL CALCULATIONS

Available on request from Risø Library, Risø National Laboratory, (Risø Bibliotek, Forsøgsanlæg Risø), P.O. Box 49, DK-4000 Roskilde, Denmark.
Telephone (02) 37 12 12, ext. 2262. Telex: 43116, Telefax: (02) 36 06 09